# Landscape structure and rainstorms swing the response of recession nonlinearity

Jun-Yi Lee[1,2], Ci-Jian Yang[2,3], Tsung-Ren Peng[1], Tsung-Yu Lee[4], Jr-Chuan Huang[2]

[1]Department of Soil and Environmental Sciences, National Chung Hsing University, Taichung 402202, Taiwan
5  [2]Department of Geography, National Taiwan University, Taipei 106319, Taiwan
[3]German Research Centre for Geosciences (GFZ), Telegrafenberg, Potsdam 14473, Germany.
[4]Department of Geography, National Taiwan Normal University, Taipei 106209, Taiwan

*Correspondence to*: Jr-Chuan Huang(riverhuang@ntu.edu.tw)

**Abstract.** Streamflow recession discloses hydrological functioning, runoff dynamics, and storage status within catchments.
10  Understanding recession response to landscape structure and rainstorms can be a guidance for assessing streamflow change under climate change. Yet, the documented response direction of recession is inconsistent and diverse. This study tested how landscape structure and rainstorms regulate the response direction. We derived 260 pairs of recession rate, *a*, and nonlinearity, *b*, from power-law recession ($-dQ/dt = aQ^b$) in 19 subtropical catchments with a broad rainfall spectrum. Results showed that the recession rate increases with the drainage density and *L/G* ratio (flow-path length over gradient), indicating that the
15  catchments with the dense network or more short-and-gentle hillslopes would result in high rates. Apart from landscape structure, the rate surprisingly decreases with rainfall amount. Probably because rainstorm facilitates connectivity in the saturated zones, which might conjoin more water from slow reservoirs and thus water drains slowly. Additionally, the recession nonlinearity increases with spatial heterogeneity (drainage area) but decreases with hillslope hydraulics (drainage density). The swing of response direction, which lies in the predominance between spatial heterogeneity and hillslope hydraulics, needs
20  further clarification, particularly for regional recession assessment under climate changes. Incorrect response direction from landscape structure would lead to considerable bias inference.

## 1 Introduction

Streamflow recession reflects a rainfall-runoff process in the falling segment of hydrograph during the rainstorm. Recession is associated with runoff paths within landscape and is critical for baseflow estimation (Palmroth et al., 2010). Previous studies
25  analyzed aggregated long-term data to retrieve recession parameters (e.g., Brutsaert and Nieber, 1977), but parameters from individual events can elucidate the recession characteristics of catchments (Jachens et al., 2020) and shed insight into the sensitivity of catchments to rainstorms that provides valuable information for water resource management under rainfall intensification. Therefore, recent studies have shifted to investigate recessions from individual events (Biswal and Nagesh Kumar, 2014; Jachens et al., 2020). It is crucial because the frequency and intensity of 10-year return period rainfall will

30   increase 1.7 times and 14%, respectively (under global warming level of 2 °C, by the Intergovernmental Panel on Climate Change, Seneviratne et al., in press).

A power-law relationship between streamflow declines with streamflow rates ($-dQ/dt = aQ^b$) can describe the recession characteristics at the catchment scale, since Brutsaert and Nieber (1977), henceforth referred to as B&N. Here, the coefficient $a$ refers to recession rate, and exponent b represents the nonlinearity of storage. Both recession parameters depend on hydraulic
35   properties (e.g., hydraulic conductivity and soil porosity), landscape structure, and rainstorms. Since the aquifer in various landscape units (e.g., hillslope, riparian, stream) exhibits different hydraulic properties, landscape structure, which presents the geometry of catchments and aggregates catchment hydraulic properties, apparently reflects various recession parameters. For example, recession rate, $a$, has a positive correlation with drainage density (Brutsaert and Nieber, 1977; Zecharias and Brutsaert, 1988) and total stream length (Bogaart et al., 2016), but has a negative correlation to flow-path length and flow-path
40   height (Bogaart et al., 2016; Karlsen et al., 2019). On the other hand, nonlinearity, $b$, increases with catchment area (Clark et al., 2009; McMillan et al., 2014) and hillslope height (Karlsen et al., 2019). Although most literature indicated that landscape structure controls the general or seasonal pattern of recession, few studies investigated the role of landscape on recession characteristics with various rainstorms.

The influence of rainstorms on recession parameters is complicated and inconsistent. Several empirical studies found a
45   positive or independent relationship between recession rate and rainfall amount (Bogaart et al., 2016) streamflow rate (Santos et al., 2019), whereas a theoretical work found that the increasing  steady state recharge rate could either enhance or reduce recession rate, depending on the spatial heterogeneity (Harman et al., 2009). On the other hand, rainfall amount corresponded negatively (Shaw, 2016) or insensitively to nonlinearity (Biswal and Marani, 2010; Brutsaert and Nieber, 1977; Dralle et al., 2017), but antecedent wetness was positive (Harman et al., 2009; Jachens et al., 2020). The various responses from literature
50   implying the control of landscape structure and rainfall amount on recession in different regions should be improved. Due to frequent tropical cyclones (alias: typhoon) and mountainous landscapes, Taiwan's river lead to short water travel time and limit water retention capacity in catchments (Lee et al., 2020). Most typhoon rainwater falls in summer and elevates water level dramatically but diminishes quickly within 2-3 days (Huang et al., 2012). Understanding the recession behaviors after typhoons are vital to water resource management, particularly when global warming likely increases the frequency and
55   magnitude of flood and drought (Shiu et al., 2012; Huang et al., 2014).

This study investigated the recession parameters along with the different magnitude of typhoons on steep landscape in the hope of identifying the interactive role of climatic and physiographic variables in recession. Specifically, we derived the recession rate and nonlinearity in 19 mountainous catchments (drainage area varies between 77–2,089 km$^2$) across Taiwan with multiyear records of hourly streamflow (260 catchment-events in total). The following questions are addressed: (1) what
60   are the recession characteristics in subtropical mountainous catchments? (2) how do climatic and physiographic variables affect recession parameters? We documented the spatial patterns of recession characteristics in Taiwan (Sect. 3) and then discussed how the recession behaviors change in different landscape settings (Sect. 4). Finally, we proposed a hypothesis: landscape structure could swing recession responses to rainstorms.

## 2 Material and methods

65 ### 2.1 Study area

Taiwan is geographically located at the juncture between the Eurasian and Philippine tectonic plates and climatologically located at the corridor of typhoons. The active mountain belt with frequent typhoons shapes steep and fractured landscapes with verdant forests. The mean annual rainfall is about 2,510 mm, and approx. 40% of annual rainfall is brought by typhoons in a few days. The lowest mean annual temperature is approx. 4°C in montane regions and 22°C in plain regions. In this

70 mountainous island, the uplifting elevation (0–4,000 m) within a short horizontal distance (~75 km) shows the steepness of the terrain feature (Huang et al., 2016). Specifically, the drainage area of most catchments is smaller than ~500 km$^2$ and stream lengths are less than ~55 km, indicating a short water travel time. The basic catchment descriptions could refer to Table S1.

Land cover inventories from the Taiwan Ministry of the Interior (www.moi.gov.tw) were reclassified from the original 13 categories into three major categories; namely, water, forest, agriculture, and others for each catchment. The landscape metric

75 describes the landscape variables which were retrieved from the digital elevation model (DEM) with 20m resolution. The specific variables and their definitions in the metric were referred to Table S1. Notably, the flow-path length ($L$), height ($H$), and gradient ($G$) above the nearest channel were retrieved by the hydrology toolset in ArcGIS 10.7, which helps to discuss how landscape control on streamflow recession (e.g., Zecharias and Brutsaert, 1988; Bogaart et al., 2016; Jachens et al., 2020).

Streamflow in this steep mountainous island usually descends quickly after a considerable surge by a typhoon. Thus, hourly

80 streamflow records are required to describe the entire streamflow recession since it only lasts a few days after peak. This study selected hourly streamflow records during 1986-2014 from the Taiwan Water Resource Agency (www.wra.gov.tw) and Tai-Power Company (www.taipower.com.tw). Only the catchments without large water division infrastructures in the upstream area and the total rainfall larger than 30 mm were used to prevent human manipulation on streamflow and guarantee the discharge rise. Based on the criteria, nineteen catchments and 260 events were filtered for further recession analysis.

85 Commensurate with the hourly streamflow, the hourly rainfall dataset from the Taiwan Central Weather Bureau (www.cwb.gov.tw) was introduced to Thiessen weighted method for areal rainfall estimation to the corresponding catchments. Collectively, a hydroclimate metric of rainstorm and streamflow presented total event rainfall, duration, average and maximum rainfall intensity, total streamflow, peak flow, and initial flow is shown in Table S2.

### 2.2 Recession analysis

90 As most analyses of hydrological processes do, the water balance equation is primarily described as Eq. (1):

$$\frac{dS}{dt} = P - E - Q$$

(1)

where $S$ is the storage volume within a catchment (in units of volume [L$^3$] or depth [L]), and $P$, $E$, and $Q$ are the rates of precipitation [L], evapotranspiration [L], and stream discharge [L$^3$/T] or [L/T], respectively. For solving the unknown storage,

95 which cannot be measured directly, all terms should be identified. The B&N formula, $Q = mS^n$ with constant $m$ and $n$ (Vogel

and Kroll, 1992), which follows Dupuit-Boussinesq, can be used to derive the relationship between storage and stream discharge. In this regard, $S$ can be replaced by $Q$ to infer the storage changes. During the recession period, $P$ and $E$ are relatively small compared to $Q$, and then the following equation is derived to represent the recession behaviors within a catchment.

$$-\frac{dQ}{dt} = nm^{\frac{1}{n}}Q^{\frac{2n-1}{n}} = aQ^b$$

100

(2)

where $a$ and $b$ are constants derived from the $Q$-$S$ relation. This power-law form between $-dQ/dt$ and $Q$ indicates that the rate of streamflow decline is highly relevant to $Q$ during the recession and has been widely plotted as "recession plot" (Kirchner, 2009). This plot enables the analysis of streamflow recessions collectively or event-independently and facilitates the derivation of storage–outflow relationships (Stölzle et al., 2013). Although the B&N formula and recession plot are widely used for

105 describing the recession behavior, the calculation procedures of recession extraction and parameter estimation are diverse due to different practical operations. For example, Stölzle et al. (2013) compared three recession extraction methods in conjunction with their corresponding parameter estimations and all possible combinations. They found that recession characteristics like recession time ($1/a$) varied over 1–2 orders of magnitude, yet exponent $b$ differed rather narrowly. Their results suggested that the recession characteristics derived with different procedures have only limited comparability and highlight the distinctiveness

110 of individual procedures due to different purposes and philosophies. Despite the differences among the procedures, applying the same procedure to a regional extent still captures the recession characteristics. The following subsections present the procedures used for extraction and parameter estimation.

### 2.2.1 Recession segment extraction

In the extraction procedure, two concerns should be addressed: (1) distinguishing between the early and late recession stage,
115 and (2) elimination of the unexpectedly positive increases in the recession. The early-stage (containing preceding storm and surface flow) and the late stage of recession (only dominated by base flow) are indistinguishable and usually determined subjectively based on different purposes. Some studies empirically excluded the early-stage recession from eliminating the influence of quick flow (e.g., Brutsaert, 2008; Vogel and Kroll, 1992). Some other studies used a threshold for the minimum length in extraction procedures from 2- to 10-days (e.g., Mendoza et al., 2003; Vogel and Kroll, 1992). Since the whole
120 recession segment represents the mixing recession behavior from quick and base flow interactively, we used peak flow as the beginning of the recession period. For eliminating unexpectedly positive increases in recession, several approaches have been proposed as well, for example, smoothing the hydrograph (Vogel and Kroll, 1992), discarding the segment directly (Brutsaert, 2008; Kirchner, 2009), and breaking-and-rejoining the recession segments (Millares et al., 2009). Each strategy has its advantages and disadvantages; smoothing the hydrograph could not completely erase the bulge caused by precipitation;
125 discarding the segment would lose part of recession events. Although breaking-and-rejoining the recession, too, disturbs the original streamflow records, the method maintains a better integral of a recession event.

This study focused on the entire streamflow recession and used the complete recession segment. First, we selected the whole recession period starting from the peak flow of the individual rainstorm. Later, we screened and broke down the hydrograph as an abrupt bulge emerged, erased the positive streamflow increases, and concatenated the remaining segments. This elimination procedure is quite similar to the master recession curve on a long-term scale (Millares et al., 2009). Third, data points corresponding to extremely low streamflow ($Q < 0.1$ mm h$^{-1}$) or recession ($-dQ/dt < 0.01$ mm h$^{-2}$) were excluded, due to the undetectable change in recession.

**2.2.2 Parameter fitting**

All extracted recession segments can be plotted on recession plot ($-dQ/dt$ vs $Q$) for estimation of B&N parameters. Several fitting methods have been proposed in the literature. First, it fits with the lower envelope of the point-cloud (Brutsaert and Nieber, 1977) since the evapotranspiration effect in a recession would lead to a higher value of $-dQ/dt$. Taking the lower envelope can prevent the evapotranspiration effect. Secondly, it fits with the entire point-cloud (Brutsaert, 2005; Vogel and Kroll, 1992) as subsoil heterogeneity may overshadow the evapotranspiration effect in larger or steeper catchments (Brutsaert, 2005). Thirdly, it fits with the binned means weighted by the square of the standard error of each binned mean (Kirchner, 2009) because the lower values of $-dQ/dt$ could be affected by the measurement errors in the streamflow observation. Recently, a virtual experiment study suggested that it is unsuitable to represent a general picture through fitting with a group of data clouds (aggregated dataset) because the preceding flow can be superimposed on the event flow, resulting in underestimation of nonlinearity (Jachens et al., 2020). In contrast, fitting with individual recession segments can capture the recession characteristics and offer an opportunity for exploring the impacts of rainstorm properties on recession. We therefore used each recession segment and fitted it with the B&N formula individually. Notably, the ordinary least square method is used to obtain estimates of parameter $a$ and $b$, but the two parameters are interactively dependent, particularly when the number of points is huge.

**3. Results**

**3.1. Recession parameters from individual and point-cloud fit**

After proceeding with the mentioned analysis onto this dataset, we demonstrated the recession plots of W5, W8, and W18 in Fig. 2. The three catchments have distinct differences in landscape, particularly in *L/G* (ratio of median flow-path length to median flow-path gradient to stream) and *ELO* (elongation), seeing Table 1. Catchment W8 has a higher *L/G* (1109) and elongated shape (low *ELO*=0.73), whereas W18 has a lower *L/G* and large *ELO*, indicating an oval shape. In descending order, the ranking of median recession rates is catchment W8, W18, and W5. As for recession exponents, the mean and median nonlinearity of W8 are 1.47 and 1.60, respectively. The three median recession rates are higher than the corresponding mean recession rates that indicate the three distribution of nonlinearity, *b*, are right-skewed (Fig. 2c). Notably, the nonlinearity

decreases with the storm magnitude in W8, yet, W5 presents an inverse pattern (Fig. 2b and 2c). The opposite responses of W8 and W5 to storm magnitude coincide with the difference of landscape variables (e.g., $L/G$) between W8 and W5.

Further, the frequency distributions of the fitted recession rate and nonlinearity of the total catchment-event records are shown in Figure 3a-b. Rate, $a$, ranges from 0.01 to 0.29 with mean = 0.076 and median = 0.043. The large difference between the median and mean shows a right-skewed distribution. Nonlinearity, $b$, ranges from 0.58 to 3.01 with mean = 1.669 and median = 1.579. The small difference between the median and mean presents an asymmetric distribution of nonlinearity. Spatial patterns of recession rate and nonlinearity are illustrated in Fig. 3c-d. Generally, larger recession rates are located in the southwestern plain (Fig. 3c). Those plain catchments also have higher $L/G$ values. Apart from this, no other distinct pattern can be found in other mountainous catchments. Conversely, the plot of recession nonlinearity presents a vague pattern (Fig. 3d), and no simple relationship could be found.

The recession parameters derived from individual segments and aggregated point-cloud data are illustrated in Fig. 4. The parameters from the individual segment which demonstrates the recession responses to each event, present the holistic variation, whereas the parameters from the aggregated point-cloud (all recession segments in the specific catchment) show the general recession behavior in that catchment. The median of the rate, $a$, increases from 0.033 to 0.121 with a catchment area of 140 km$^2$ and decreases to about 0.016 with catchment area above 800 km$^2$ and the interquartile ranges are pretty large in catchments with the mid-sized area between 140 (W14) and 220 km$^2$ (W12). On the other hand, the medians of $a$ from the aggregated point-cloud fits fall in the interquartile range of the individual fit distribution, indicating that the recession rates only lightly change between the fitting methods. The median and interquartile of nonlinearity from individual segments irrelative to catchment area, and the values from the aggregated point-cloud are consistently lower than that from individual segments except W19. Besides, about half of nonlinearity, $b$, from the aggregated point-cloud are outside the interquartile range of the distribution. Considerable difference between the two fitting methods brings about the difficulty in comparison and inference. The details of the recession characteristics for each catchment can be referred to Table S3.

## 3.2 Recession parameters to event characteristics

The correlation coefficients of recession parameters to event-associated variables are shown in Fig. 5 and Table 1 to capture how hydrometric forcing affects recession. The total precipitation ($P$), duration ($D$), total streamflow ($Q_{tot}$), initial streamflow ($Q_{ini}$) and runoff coefficient ($Q_{tot}/P$) are negatively correlated to the recession rate, $a$. The average precipitation intensity ($I_{avg}$) and peak flow ($Q_p$), both of which represent the strength of rainstorm, are not significant to rate, $a$. As for initial conditions, the 7-day antecedent precipitation, $AP_{7day}$, is not correlated to the rate, $a$; other lengths of $AP$ (3-, 5-, 14-, and 30-day) also show insignificant correlation to the rate, $a$. Collectively, $Q_{ini}$ is negatively correlated to the rate, $a$.

Unlike recession rate, $a$, which strongly depends on the hydrometric variables, nonlinearity, $b$, is only positive to $Q_{ini}$. Higher initial flow could lead to higher nonlinearity. What is surprising is that no rainfall or flow variables are associated with the nonlinearity, which contradicts the presumed thoughts and will be discussed in the next section. To summarize from the view of the aggregated dataset, hydrometric forcing moderately controls the rate and only slightly involves nonlinearity.

### 3.3 Recession parameters to landscape variables

On our 19 catchments, average height ($H$), length ($L$) and gradient ($G$) of flow-path are approx. 120m, 252m and 0.47, respectively (Table S1). The $L/G$, regarded as a proxy presenting interaction of landscape and climate, is approx. 951m. Forest is the dominant landscape, and the average forest coverage is approx. 67.1% with a range between 11.8-92.1%. Notably, the catchments in the western plain are characterized by gentle gradients of flow-path, such as catchments W8, W9, W11, W12, W13, and W14. Due to the gentle landscape and higher $L/G$, agricultural activities are the dominant land cover in those catchments. The details of landscape variables could be referred to Table S1.

The correlations between recession parameters against event and landscape variables are illustrated in Fig. 5 and Table 1. Most landscape variables ($H$, $L$, $G$, $L/G$, $DD$, $S_m$, $HI$, $C_W$, $C_F$, and $C_A$) are significantly correlated to the rate, particularly for the flow-path-associated ones ($H$, $L$, $G$, $L/G$, and $DD$). Note that flow-path-associated variables, such as flow-path height ($H$), length ($L$), and gradient ($G$), are negatively correlated to $L/G$ and $DD$. Besides, the rate increases with the decrease of $S_m$, indicating that quick recession occurs in a mainstream with a gentle gradient. In contrast, the rate increases with $HI$, showing a sharp recession in actively eroded catchments. Moreover, the rate increases with $C_W$ (fraction of water body area) and $C_A$ (fraction of agriculture area) and decreases with $C_F$ (fraction of forest area). Results illustrate that a catchment with more water bodies and agricultural lands leads to a faster recession, yet a catchment with more forest lands could reduce the recession rate. In short, most landscape variables are highly associated with the rate and only a few, such as $HI$ and $A$ are slightly negative to the nonlinearity. Yet, putting all catchments with various landscape features together may obscure the landscape control in recession rate and nonlinearity.

## 4. Discussion

### 4.1 Recession parameters in subtropical mountainous catchments

The range of recession rate from our 19 catchments is 0.010 to 0.290, comparable with values in the literature, for example, 0.012 to 0.230 for Swedish catchments (Bogaart et al., 2016) and 0.015 to 0.171 for USA watersheds (Biswal and Marani, 2010). Higher median recession rates are found in W8, W11, W12, and W14, where shorter-, steeper- flow paths and dense drainage networks are the main landscape features. By contrast, catchments with longer-, gentle-flow paths and sparse drainage networks, such as W7 and W15, have lower median recession rates. It implies that landscape structure (e.g., drainage density and flow-path-associated variables) could affect the recession rate. On the other hand, the median of recession nonlinearity, $b$, is approx. 1.6 (Fig. 3b) with a range of 0.6 to 3.0, which are also comparable with the ranges in the literature. For example, values of $b$ from 0.5 to 2.1 could be found in 220 Swedish catchments with low flow data (Bogaart et al., 2016), 0.6 to 1.7 for 22 Taiwanese rivers derived from low-flow data (Yeh and Huang, 2019), and 1.5 to 3.2 for 67 USA watersheds with event data (Biswal and Marani, 2010). Nonlinearity higher than 1.0 indicates non-linear storage–outflow relationship, typical for most catchments worldwide. In our cases, the highest and lowest median nonlinearity is in W7 and W19, respectively.

Catchment W7 with high channel slope and flow-path gradient (Table S1), presents higher non-linear storage-outflow. W19, by contrast, has the similar landscape settings with W7, but has the lowest. Other controlling factors, such as geological structure or land cover, might dominate the recession behavior (Tague and Grant, 2004).

225     Notably, a distinct systematic bias is found between the nonlinearity derived from individual segments and the aggregated point-cloud (Fig. 4). Smaller $b$ value derived from the aggregated point-cloud than that from individual segments could be expected since the flood distribution is right-skewed; that is, large number of small cases with scarce extremes. Nonlinearity $b$ derived from aggregated point-cloud is synthesized from all points, which could be altered either by the numerous small cases or the scarce extreme cases as fitting. The median from aggregated point-cloud is more or less like the way in the master recession curve. Jachens et al. (2020) indicated that the event properties (variation among inter-event, storm magnitude, and

230 antecedent condition) strongly affect the parameter estimation. In this regard, it suggested that using the median from individual segments to represent the central tendency of a collection of recession segments is a better way to obtain the representative recession properties (Dralle et al., 2017; Jachens et al., 2020).

## 4.2 Landscape structure controls the median of recession parameters

Landscape structure aggregates catchment hydraulic properties, embodying recession parameters conceivably. On the other

235 hand, recession behaviors in a catchment can be interpreted from two perspectives: hillslope hydraulics and hillslope heterogeneity (Harman et al., 2009), both of which are highly relevant to landscape structure, notably the flow-path-associated variables (e.g., $H$, $L$, $G$, $L/G$, $DD$ in Table 1), which describe hillslope hydraulics by addressing the distance and gradient of flow to the stream. Further, a catchment area generally complicates the heterogeneity of a hillslope and consequently increases the recession nonlinearity. Two studies, for example, investigated the recession behaviors in two small forested catchments

240 (68 km$^2$ in Mahurangi, New Zealand, McMillan et al., 2014 and 41 ha in Panola Mountain Research Watershed, USA, Clark et al., 2009; Harman et al., 2009) and found that recession nonlinearity increases with catchment area because a larger area accommodates more possibility of superimposition of multiple linear reservoirs.

    Correlation analysis elucidates that flow-path-associated variables ($H$, $L$, $G$, $L/G$, $DD$) dominate the recession rate. The southwestern catchments marked by low gradient have higher recession rates (Fig. 3c); however, in our cases, most landscape

245 variables only have a vague correlation with the recession nonlinearity (Fig. 6a). It might be explained by: first, some of our catchments are much larger than 500 km$^2$, which exceeds the extent of common rainstorms (usually less than 200 km$^2$). In those large catchments, the limited extent of rainstorm would not induce a complete recession process in the outflow hydrograph (Huang et al., 2012). Second, catchment area cannot reflect the unknown number of aquifers (Ajami et al., 2011). Moreover, Karlsen et al. (2019) argued that the dependence of landscape variables would change with streamflow rate.

250 Specifically, the $H$ dominates the nonlinearity during high flow, whereas the catchment area gains more importance during low flows. Therefore, the relationship between hillslope hydraulics and spatial heterogeneity with recession needs to be further examined in our catchments. Besides, since catchment area could not sufficiently explain the recession behaviors (Fig. 6a), we try including flow-path-associated variables to estimate the recession parameters.

### 4.2.1 Landscape structure to recession rate, *a*

255    In trying all flow-path-associated indices to correlate with catchment area, we found that the *L/G* ratio presents an inverse relationship against catchment area (Fig. 6b). The *L/G* ratio is a measure of the distribution of flow-path length over gradient at a catchment scale (McGuire et al., 2005), which is correlated to *DD* and the topographic wetness index (Beven and Kirkby, 1979). The *L/G* or *DD*, therefore, can present the hillslope hydraulics at a catchment scale. In this regard, the catchments can be classified from two dimensions (Fig. 6b); namely, the heterogeneity, in which Type B to A is from small to large area, and

260    the hydraulics dimension, from Type B to C is from low to high *L/G*. Based on the classification, the flow-path-associated variables (*H*, *L*, *L/G*, and DD) are highly correlated to the recession parameters (Fig. 7). *H* is directly linked to the water table depth under the relatively homogeneous hillslopes. Hence, steeper hillslope corresponds to permeable soils with higher *H*, leading to a deeper and longer groundwater flow system and slower drainage (Karlsen et al., 2019). The high *DD* (Brutsaert and Nieber, 1977) and short *L* (Zecharias and Brutsaert, 1988) lead to a quick recession rate due to shorter flow paths.

265    Additionally, McGuire et al. (2005) demonstrated isotopic evidence to prove that the transit times increase with *L* in Oregon, USA. In our case, both *DD* and *L/G* (Fig. 7a-c) confirm the documented relationships. Catchments with high *DD* or *L/G*, which represent a denser stream network or short-and-gentle hillslopes, have a higher recession rate.

### 4.2.2 Landscape structure to recession nonlinearity, *b*

The recession nonlinearity conditionally responds to landscape structure (Fig. 7e-7h). If Type A catchments (large area with

270    low *L/G*) are excluded, meaning only the hydraulics dimension is considered. All flow-path-associated variables become statistically significant for the estimation of nonlinearity. The positive relationship with *H* and *L* indicates that steeper and rougher hillslopes tend to divert water to temporarily store behind blocks, leading to a non-linear recession behavior. The two composite indices, *DD* and *L/G*, are negatively related to the value of *b* (Fig. 7g-h). Short-and-gentle hillslopes, which lead to a larger saturation area nearby the riparian zone as rainfall, reduce the degree of heterogeneity in drainage behavior. By

275    contrast, lower *DD* characterized by longer subsurface flow systems has a higher value of *b* (Bogaart et al., 2016; Sayama et al., 2011). It suggested that hillslope hydraulics dimension (*DD* and *L/G*) affects the nonlinearity significantly, but it was only valid within catchment size less than 500km$^2$.

### 4.3 Rainfall amount controls the variation of recession parameters

Recession behavior is a convolutional response starting from rainfall amount hitting the catchments. The large deviation in a

280    fixed catchment (Fig. 7) presented the role of rainfall amount (hydrometric variables) in recession behaviors (Biswal and Nagesh Kumar, 2014). Thus, we separately examined the recession parameters against hydrometric variables for the three catchment types to rule out the influences (Fig. 8). Two significant findings are: (1) the recession rate decreases with the rainfall amount in all types; (2) the recession nonlinearity shows opposite responses in Type A and C (Type B is statistically

insignificant). The parameter, *b*, in heterogeneity-dominated or hydraulics-dominated catchments would increase or decrease

285  with rainfall amount, respectively. In other words, landscape structure dominates the response direction of recession.

### 4.3.1 Rainfall amount on recession rate, *a*

Several empirical studies found a positive or independent relationship between rate, *a* and streamflow; for example, Santos et al. (2019) found that higher streamflow has a larger rate, reflecting a quick recession in Switzerland catchments. In Sweden, annual rainfall variation might be independent of the rate (Bogaart et al., 2016). By contrast, Harman et al. (2009) designed a

290  virtual experiment that theoretically considered the recession response corresponding to spatially-heterogeneous storages. They assumed that the flow velocities of a catchment, organized by a series of hillslope with individual linear reservoirs, can be represented by a probability density distribution (pdf, e.g., Gamma distribution). Thus, the outflow and recession parameters could be evaluated by the recharge rate convolving with instantaneous unit hydrographs. Theoretically, the recession rate is determined by the tension between the recharge rate with spatial heterogeneity of storage and flow velocity. In this regard,

295  increasing recharge rate could reduce the recession rate. On the other hand, recharge rate also indirectly increases flow velocity and then enhances the rate, *a*. Therefore, the influence of rainfall amount presents various response directions in real catchments.

Recession rate in our three catchment types reduces with rainfall amount (Fig. 8a-c). Therefore, the influence of rainfall amount in our catchments overwhelms the effect of flow velocity, resulting in a slower recession in large rainstorms.

300  Additionally, the significant decrease in Type C catchments (higher *DD* or short-and-gentle catchments) is likely because that, with the rainfall increase, saturated zones connect more water from slow reservoirs resulting in slow water drainage.

### 4.3.2 Opposite control of rainfall on recession nonlinearity, *b*

The dependence of recession nonlinearity on rainfall is divergent. It has been documented as insensitive, negative or positive in various literature. Some studies concluded that nonlinearity, *b*, is controlled by landscape structure and is static or is

305  insensitive to rainfall (Biswal and Marani, 2010; Brutsaert and Nieber, 1977; Dralle et al., 2017). In other studies, nonlinearity, *b*, decreases with streamflow rate on different temporal scales (Shaw and Riha, 2012; Karlsen et al., 2019; Santos et al., 2019). In our study, nonlinearity *b* presents a positive, flat, negative relationship with rainfall in Type A, B, and C catchments, respectively (Fig. 8d-f). A possible interpretation is that the short-and-gentle catchments (Type C catchments) have a wide range of contributing area, which expands with rainfall quickly. The pervasive saturation overland flow reduces the

310  nonlinearity of recession. Besides, large rainstorms also can connect saturated zones from slow reservoirs (e.g., hillslope or low hydraulic conductivity region) and thus drain water slowly. On the contrary, the nonlinearity, *b*, increases with the rainfall amount in Type A catchments. In large and heterogeneous catchments, the expansion of contributing area is more unsteady and complicated, and thus the nonlinearity increases with rainfall amount. The nonlinearity increases with the heterogeneity of catchment properties (Harman et al., 2009).

### 4.4 Landscape structure regulates recession patterns

The above two sections elucidate that landscape structure controls the response direction of recession (the median recession parameter), whereas rainfall amount influences the responsive degree of recession behaviors. Thus, a hypothesis that demonstrates the interactive regulation of landscape structure and rainfall amount on recession nonlinearity is introduced (Fig. 9). Landscape structure is considered from two dimensions in terms of spatial heterogeneity and hillslope hydraulics, which are, respectively, represented by drainage area and *DD*. While the drainage area might correlate to the number of perched storages within the catchments, the *DD* featured by short-and-gentle hillslope indicates that the size of contributing area dominates the runoff generation mechanism.

Along spatial heterogeneity dimension (from Type B to A, with increasing drainage area), additional perched storages respond increasingly with rainfall amount and thus enhance the recession nonlinearity. Perched storages are inclined to occur where the hydrological conductivity abruptly decreases due to heterogeneous soil properties or geological structure. Large catchments tend to have more perched storages, and consequently uneven spatial rainfall activate perched storages locally, and thus, the nonlinearity increases. On the other hand, along the hillslope hydraulics dimension (from Type B to C, with increasing *DD*), the accumulated rainfall expands saturation zone quickly, which prefers the generation of saturation excess overland flow. With the increase of *DD*, the runoff generation mechanism varies from unpredictable subsurface runoff to overall saturation excess overland flow, and thus decreases nonlinearity.

### 5. Summary

Streamflow recession, which reflects the rainfall-runoff process after rainstorms, is crucial for baseflow estimation and assessment. This study investigated the recession responses to landscape structure and rainfall amount through power-law recession from 260 catchment events. Despite the power-law equation being widely used, the procedure of parameter estimation is diverse and has brought about considerable inconsistency. For example, selecting the recession segment from peak flow might derive higher nonlinearity, and using the whole point-cloud data might underestimate the nonlinearity at the event scale. The determination and selection of recession segments predominate the rate and nonlinearity significantly and lead to controversy, which makes the inter-comparison among studies complicated and delivers biased inference.

Several studies have demonstrated the effect of landscape structure and rainfall amount on recession parameters, yet the results are pretty diverse. In our cases, landscape structure, mainly *DD* or *L/G*, and rainfall amount play dominant roles in estimating recession rate. The rate increases with the increase of *DD* or *L/G*, indicating catchments with dense networks or more short-and-gentle hillslopes would lead to a higher rate. Surprisingly, it decreases with rainfall amount; probably the large rainfall develops saturated zones connectivity, resulting in more water from slow reservoirs and drained slowly. This conceptual interpretation or hypothesis needs further validation. The diverse response direction of nonlinearity likely depends on spatial heterogeneity (drainage area) and hillslope hydraulics (drainage density), respectively. The more heterogeneous catchments give rise to the increase in the recession nonlinearity. On the contrary, catchments with higher hillslope hydraulics

could expand contributing area easily, and then generate saturation overland flow pervasively and thus reduce recession nonlinearity. Conjointly, our hypothesis presents an interactive regulation of landscape structure and rainfall amount to recession. In sum, landscape structure which has different preferences of recession mechanism, and the rainfall amount tunes
350    the magnitude of recession nonlinearity apparently. If the hypothesis is valid, two challenges should be addressed further. First, the alteration of response direction lies in the predominance between spatial heterogeneity and hillslope hydraulics. Clarifying which factors could present the spatial heterogeneity and hillslope hydraulics is an arduous task but is helpful for recession estimation. Second, the determination of response direction is crucial to the regional recession assessment, particularly for climatic scenarios. The incorrect direction would strongly affect the inference. Validating the landscape structure control in
355    different regions would aid in completing the recession variations.

*Data availability.* Hourly streamflow data can apply in Taiwan Water Resource Agency and Tai-Power company. The authors declare that data supporting the findings of this study are available within the article and its supplementary materials.
360

*Author contributions.* Conceptualization and Methodology: JYL and JCH. Data Curation and Validation: TYL. Formal analysis: JYL and CJY. Investigation and Writing – Original Draft: JYL. Writing – Review and Editing: JCH and TRP.

*Competing interests.* The authors claim no potential competing interests
365

*Acknowledgements.* This research was funded by the Ministry of Science and Technology, Taiwan (110-2811-M-005-509, and 109-2811-B-002-631) and the NTU Research Center for Future Earth (107L901004). J. Y. Lee and C. J. Yang was supported by the grants from Ministry of Science and Technology, Taiwan (110-2811-M-005-521, 110-2917-I-564-009).

# References

Ajami, H., Troch, P. A., Maddock III, T., Meixner, T., and Eastoe, C.: Quantifying mountain block recharge by means of catchment-scale storage-discharge relationships, Water Resour. Res., 47, W04504, https://doi.org/10.1029/2010WR009598, 2011.

Beven, K. J. and Kirkby, M. J.: A physically based, variable contributing area model of basin hydrology, Hydrol. Sci. J., 24, 43–69, https://doi.org/10.1080/02626667909491834, 1979.

Biswal, B. and Marani, M.: Geomorphological origin of recession curves, Geophys. Res. Lett., 37, L24403, https://doi.org/10.1029/2010GL045415, 2010.

Biswal, B. and Nagesh Kumar, D.: Study of dynamic behaviour of recession curves, Hydrol. Process., 28, 784–792, https://doi.org/10.1002/hyp.9604, 2014.

Bogaart, P. W., Van Der Velde, Y., Lyon, S. W., and Dekker, S. C.: Streamflow recession patterns can help unravel the role of climate and humans in landscape co-evolution, Hydrol. Earth Syst. Sci., 20, 1413–1432, https://doi.org/10.5194/hess-20-1413-2016, 2016.

Brutsaert, W.: Hydrology: an introduction, Cambridge university press, https://doi.org/10.1017/CBO9780511808470, 2005.

Brutsaert, W.: Long-term groundwater storage trends estimated from streamflow records: Climatic perspective, Water Resour. Res., 44, W02409, https://doi.org/10.1029/2007WR006518, 2008.

Brutsaert, W. and Nieber, J. L.: Regionalized drought flow hydrographs from a mature glaciated plateau, Water Resour. Res., 13, 637–643, https://doi.org/10.1029/WR013i003p00637, 1977.

Clark, M. P., Rupp, D. E., Woods, R. A., Tromp-van Meerveld, H., Peters, N., and Freer, J.: Consistency between hydrological models and field observations: linking processes at the hillslope scale to hydrological responses at the watershed scale, Hydrol. Process. Int. J., 23, 311–319, https://doi.org/10.1002/hyp.7154, 2009.

Dralle, D. N., Karst, N. J., Charalampous, K., Veenstra, A., and Thompson, S. E.: Event-scale power law recession analysis: quantifying methodological uncertainty, Hydrol. Earth Syst. Sci., 21, 65–81, https://doi.org/10.5194/hess-21-65-2017, 2017.

Harman, C. J., Sivapalan, M., and Kumar, P.: Power law catchment-scale recessions arising from heterogeneous linear small-scale dynamics, Water Resour. Res., 45, W09404, https://doi.org/10.1029/2008WR007392, 2009.

Huang, J.-C., Yu, C.-K., Lee, J.-Y., Cheng, L.-W., Lee, T.-Y., and Kao, S.-J.: Linking typhoon tracks and spatial rainfall patterns for improving flood lead time predictions over a mesoscale mountainous watershed, Water Resour. Res., 48, W09540, https://doi.org/10.1029/2011WR011508, 2012.

Huang, J.-C., Lee, T.-Y., and Lee, J.-Y.: Observed magnified runoff response to rainfall intensification under global warming, Environmental Research Letters, 9, 034008, https://doi.org/10.1088/1748-9326/9/3/034008, 2014.

Huang, J.-C., Lee, T.-Y., Lin, T.-C., Hein, T., Lee, L.-C., Shih, Y.-T., Kao, S.-J., Shiah, F.-K., and Lin, N.-H.: Effects of different N sources on riverine DIN export and retention in a subtropical high-standing island, Taiwan, Biogeosciences, 13, 1787–1800, https://doi.org/10.5194/bg-13-1787-2016, 2016.

Jachens, E. R., Rupp, D. E., Roques, C., and Selker, J. S.: Recession analysis revisited: impacts of climate on parameter estimation, Hydrol. Earth Syst. Sci., 24, 1159–1170, https://doi.org/10.5194/hess-24-1159-2020, 2020.

405 Karlsen, R. H., Bishop, K., Grabs, T., Ottosson-Löfvenius, M., Laudon, H., and Seibert, J.: The role of landscape properties, storage and evapotranspiration on variability in streamflow recessions in a boreal catchment, J. Hydrol., 570, 315–328, https://doi.org/10.1016/j.jhydrol.2018.12.065, 2019.

Kirchner, J. W.: Catchments as simple dynamical systems: Catchment characterization, rainfall-runoff modeling, and doing hydrology backward, Water Resour. Res., 45, W02429, https://doi.org/10.1029/2008WR006912, 2009.

410 Lee, J.-Y., Shih, Y.-T., Lan, C.-Y., Lee, T.-Y., Peng, T.-R., Lee, C.-T., Huang, J.-C.: Rainstorm Magnitude Likely Regulates Event Water Fraction and Its Transit Time in Mesoscale Mountainous Catchments: Implication for Modelling Parameterization. Water, 12, 1169, https://doi.org/10.3390/w12041169, 2020.

McGuire, K., McDonnell, J. J., Weiler, M., Kendall, C., McGlynn, B., Welker, J., and Seibert, J.: The role of topography on catchment-scale water residence time, Water Resour. Res., 41, W05002, https://doi.org/10.1029/2004WR003657, 2005.

415 McMillan, H., Gueguen, M., Grimon, E., Woods, R., Clark, M., and Rupp, D. E.: Spatial variability of hydrological processes and model structure diagnostics in a 50 km$^2$ catchment, Hydrol. Process., 28, 4896–4913, https://doi.org/10.1002/hyp.9988, 2014.

Mendoza, G. F., Steenhuis, T. S., Walter, M. T., and Parlange, J.-Y.: Estimating basin-wide hydraulic parameters of a semi-arid mountainous watershed by recession-flow analysis, J. Hydrol., 279, 57–69, https://doi.org/10.1016/S0022-420 1694(03)00174-4, 2003.

Millares, A., Polo, M. J., and Losada, M. A.: The hydrological response of baseflow in fractured mountain areas, Hydrol. Earth Syst. Sci., 13, 1261–1271, https://doi.org/10.5194/hess-13-1261-2009, 2009.

Palmroth, S., Katul, G. G., Hui, D., McCarthy, H. R., Jackson, R. B., and Oren, R.: Estimation of long-term basin scale evapotranspiration from streamflow time series, Water Resour. Res., 46, W10512, https://doi.org/10.1029/2009WR008838, 425 2010.

Santos, A. C., Portela, M. M., Rinaldo, A., and Schaefli, B.: Estimation of streamflow recession parameters: New insights from an analytic streamflow distribution model, Hydrol. Process., 33, 1595–1609, https://doi.org/10.1002/hyp.13425, 2019.

Sayama, T., McDonnell, J. J., Dhakal, A., and Sullivan, K.: How much water can a watershed store?, Hydrol. Process., 25, 3899–3908, https://doi.org/10.1002/hyp.8288, 2011.

430 Seneviratne, S.I., X. Zhang, M. Adnan, W. Badi, C. Dereczynski, A. Di Luca, S. Ghosh, I. Iskandar, J. Kossin, S. Lewis, F. Otto, I. Pinto, M. Satoh, S.M. Vicente-Serrano, M. Wehner, and B. Zhou: Weather and Climate Extreme Events in a Changing Climate, in: Climate Change 2021: The Physical Science Basis. Contribution of Working Group I to the Sixth Assessment Report of the Intergovernmental Panel on Climate Change, edited by: Masson-Delmotte, V., P. Zhai, A. Pirani, S.L. Connors, C. Péan, S. Berger, N. Caud, Y. Chen, L. Goldfarb, M.I. Gomis, M. Huang, K. Leitzell, E. Lonnoy, J.B.R. 435 Matthews, T.K. Maycock, T. Waterfield, O. Yelekçi, R. Yu, and B. Zhou, Cambridge University Press. In Press.

Shaw, S. B.: Investigating the linkage between streamflow recession rates and channel network contraction in a mesoscale catchment in New York state, Hydrol. Process., 30, 479–492, https://doi.org/10.1002/hyp.10626, 2016.

Shaw, S. B. and Riha, S. J.: Examining individual recession events instead of a data cloud: Using a modified interpretation of dQ/dt–Q streamflow recession in glaciated watersheds to better inform models of low flow, J. Hydrol., 434, 46–54,
440   https://doi.org/10.1016/j.jhydrol.2012.02.034, 2012.

Shiu, C., Liu, S. C., Fu, C., Dai, A., and Sun, Y.: How much do precipitation extremes change in a warming climate?, Geophys. Res. Lett., 39, L17707, https://doi.org/10.1029/2012GL052762, 2012.

Stölzle, M., Stahl, K., and Weiler, M.: Are streamflow recession characteristics really characteristic?, Hydrol. Earth Syst. Sci., 17, 817–828, https://doi.org/10.5194/hess-17-817-2013, 2013.

445   Tague, C. and Grant, G. E.: A geological framework for interpreting the low-flow regimes of Cascade streams, Willamette River Basin, Oregon, Water Resour. Res., 40, W04303, https://doi.org/10.1029/2003WR002629, 2004.

Vogel, R. M. and Kroll, C. N.: Regional geohydrologic-geomorphic relationships for the estimation of low-flow statistics, Water Resour. Res., 28, 2451–2458, https://doi.org/10.1029/92WR01007, 1992.

Yeh, H. and Huang, C.: Evaluation of basin storage–discharge sensitivity in Taiwan using low-flow recession analysis, Hydrol.
450   Process., 33, 1434–1447, https://doi.org/10.1002/hyp.13411, 2019.

Zecharias, Y. B. and Brutsaert, W.: The influence of basin morphology on groundwater outflow, Water Resour. Res., 24, 1645–1650, https://doi.org/10.1029/WR024i010p01645, 1988.

**Table 1: Spearman correlation coefficients between logarithmic hydrometric characteristics and recession characteristics for all catchment-events (n = 260). Values in bold are statistically significant with the 99% level of confidence (p-value< 0.01).**

| Variable | $a$ | $b$ | Meaning |
|---|---|---|---|
| Hydrometric | | | |
| $AP_{7day}$ | -0.09 | 0.14 | 7-day antecedent precipitation |
| $P$ | **-0.44** | -0.00 | Total precipitation |
| $D$ | **-0.38** | -0.07 | Duration of precipitation |
| $I_{avg}$ | -0.19 | 0.07 | Averaged precipitation intensity |
| $Q_{tot}$ | **-0.52** | -0.02 | Total streamflow |
| $Q_{ini}$ | **-0.31** | **0.38** | Initial streamflow |
| $Q_p$ | -0.13 | 0.09 | Peak flow |
| $Q_{tot}/P$ | **-0.29** | 0.00 | Runoff coefficient |
| Landscape | | | |
| $H$ | **-0.62** | 0.07 | Median of flow-path height above the nearest drainage |
| $L$ | **-0.62** | 0.13 | Median of flow-path length to the nearest drainage |
| $G$ | **-0.59** | 0.03 | Median of flow-path gradient to the nearest drainage |
| $L/G$ | **0.60** | -0.04 | Ratio of flow-path length to flow-path gradient |
| $A$ | -0.05 | **-0.19** | Catchment area |
| $DD$ | **0.60** | -0.10 | Drainage density |
| $S_m$ | **-0.40** | 0.08 | Gradient of mainstream |
| $HI$ | **0.45** | **-0.23** | Hypsometric integral |
| $ELO$ | -0.12 | -0.14 | Basin elongation |
| $C_W$ | **0.36** | -0.08 | Land cover - water bodies |
| $C_F$ | **-0.39** | 0.08 | Land cover - forest |
| $C_A$ | **0.37** | -0.07 | Land cover - agriculture |
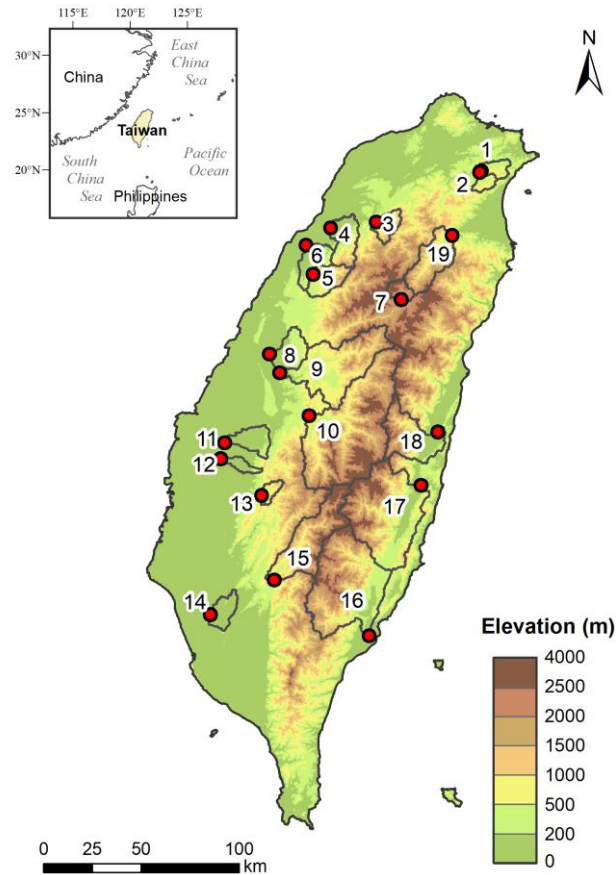
**Figure 1: Topographic distribution of Taiwan and the locations of the selected catchments. The catchment ID can be referred to Table S1 and S2, in which the primary descriptions of hydrologic events and landscape variables are listed.**
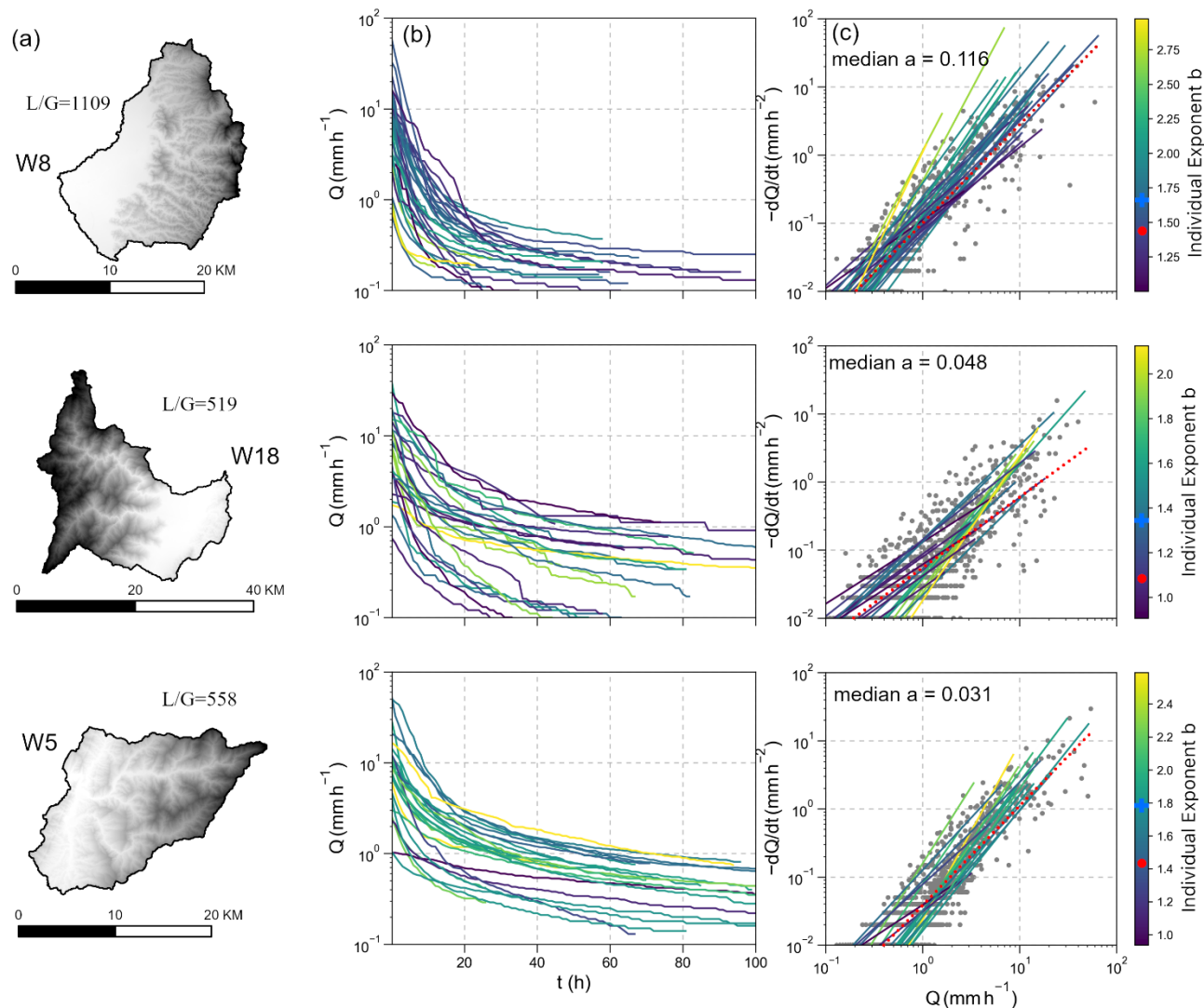
**Figure 2: Landscape and recession plots for catchment W8 (row 1), W18 (row 2), and W5 (row 3). Landscape and**
**catchment shape are shown in column (a). The selected recession segments from different rainstorms are shown in (b).**
**Recession plots with point-cloud from all selected rainstorms are shown in column (c). The median of recession**
**coefficient *a* is shown in the upper-left corner and the recession exponent, *b*, from individual segment are colored from**
**purple to yellow with increasing value of *b*. Note that the blue cross and red dot in the color bar represent the median**
**and mean of the recession exponent.**
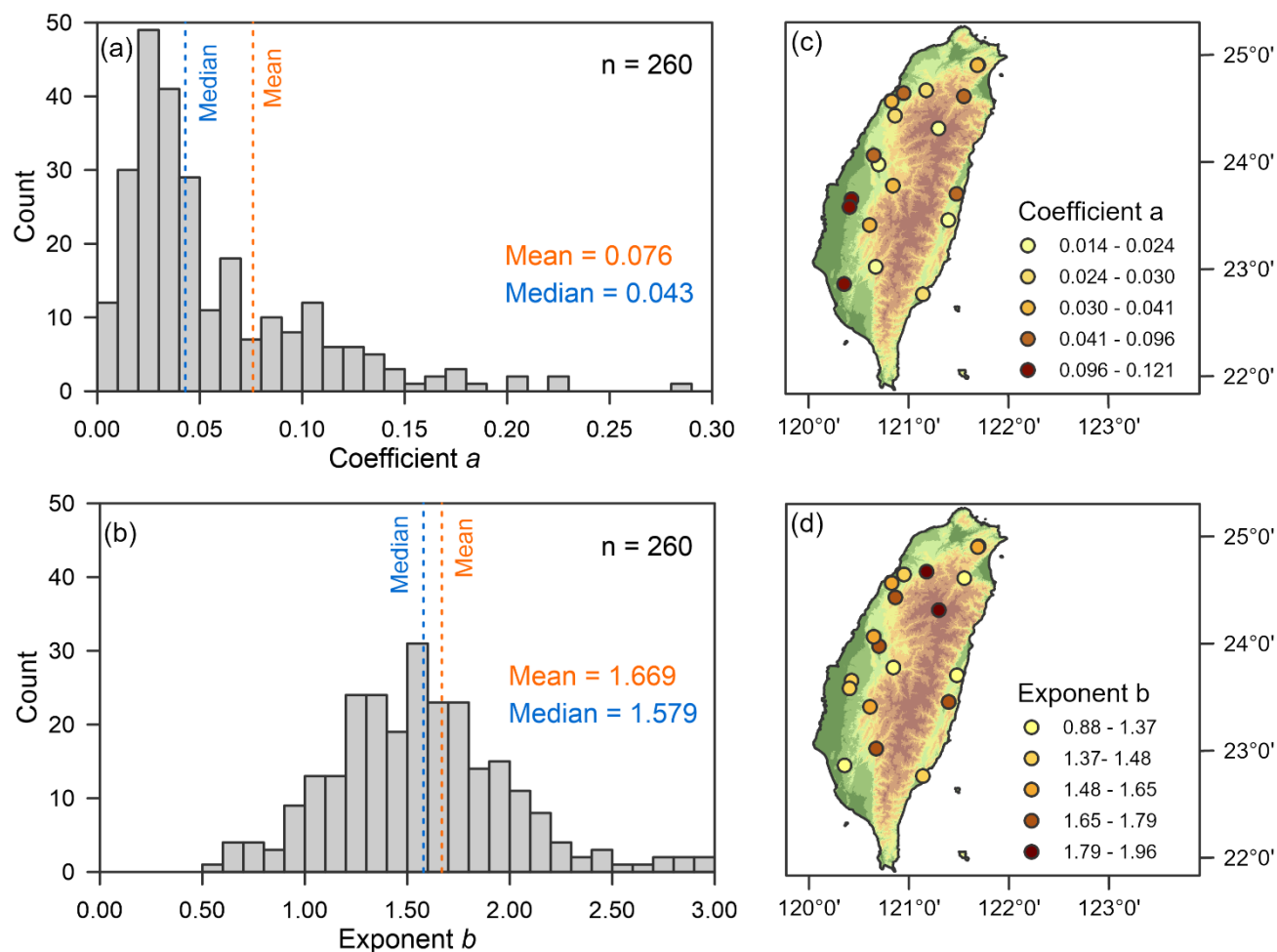
**Figure 3: Distributions of recession parameter *a* (a) and *b* (b) in all catchment-events. Spatial distributions of the medians of parameter *a* (c) and *b* (d). Colors of dot represent quantiles category.**
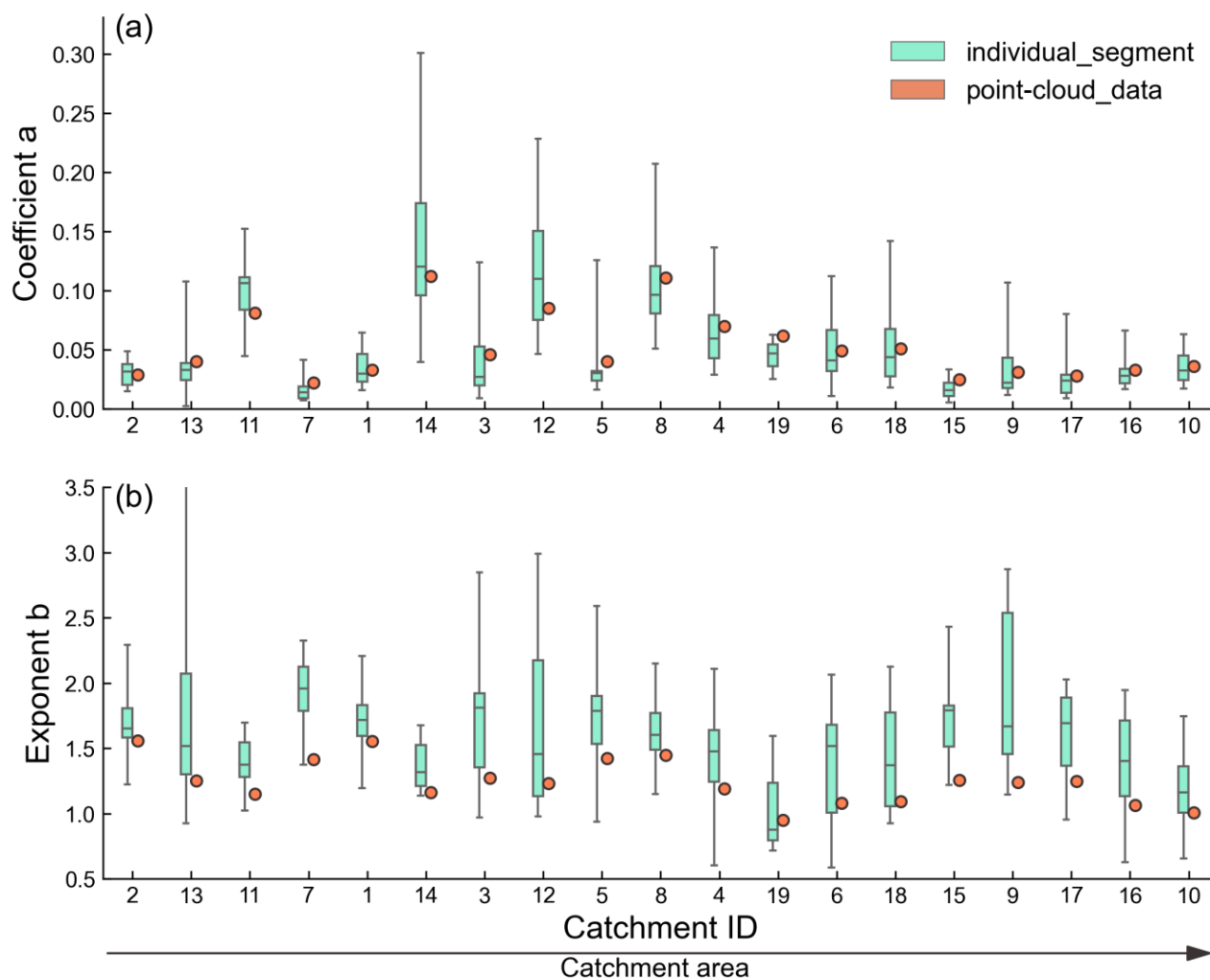
**Figure 4: Boxplots of coefficient *a* (a) and exponent *b* (b) derived from individual recession segment (cyan box) and point-cloud data (orange dot). The catchment area is used in *x*-axis in ascending order. Boxes show the interquartile and data range.**
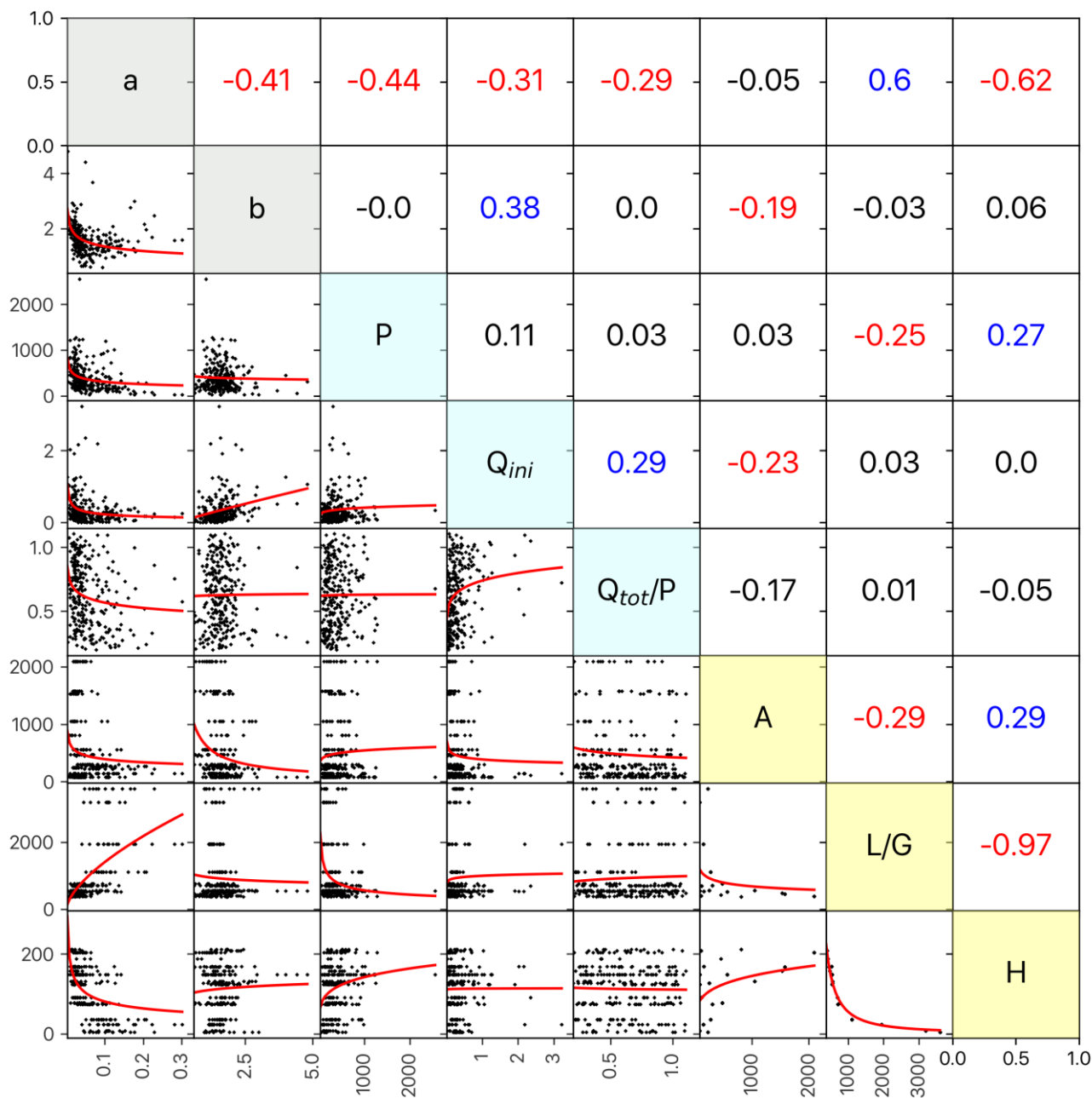
**Figure 5: Recession parameter, *a* and *b* against event and landscape variables. Below diagonal: scatter plots for recession parameters with a power-fit regression (red line). Above diagonal: corresponding Spearman correlation coefficients. Values in blue and red color are positive and negative statistically significant with the 99% level of confidence (*p*< 0.01), respectively.**
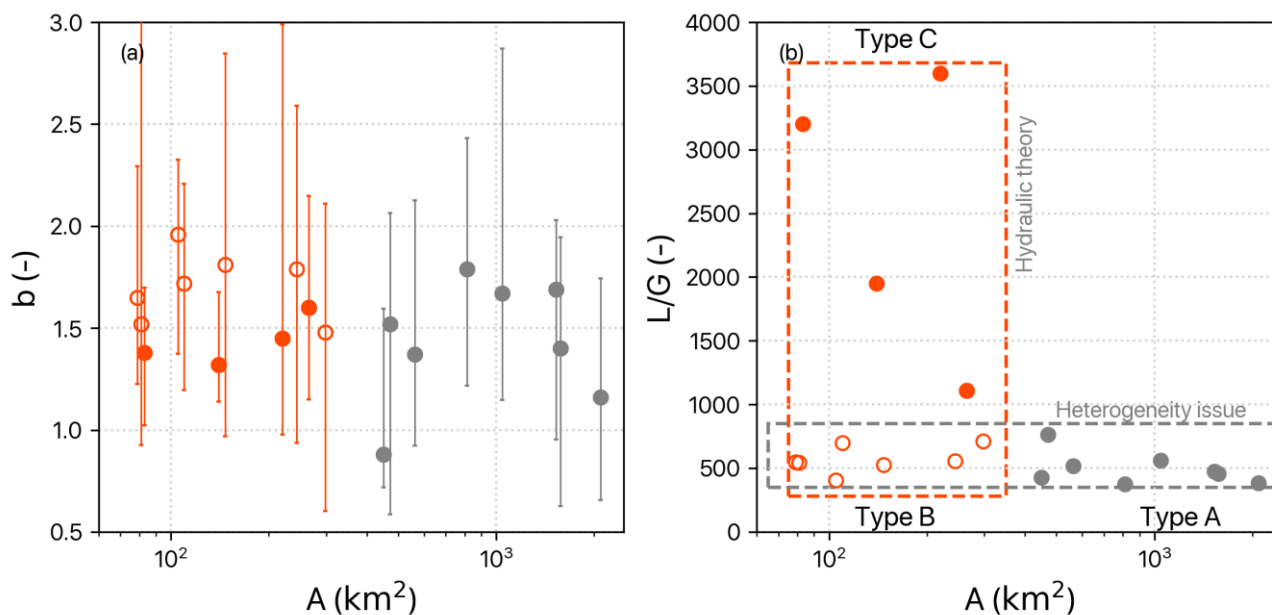
**Figure 6: The relationship between catchment area and the recession exponent (a) and the flow path topography (*L/G*) (b). The error bar on (a) is the range of the recession exponent of each catchment. The orange and gray dots represent small and large catchments, respectively. The solid and hollow dots represent large and small L/G. The recession**
490 **behaviors in small and large catchments could be explained from two perspectives in terms of hydraulic theory (orange box) and heterogeneity issues (gray box).**
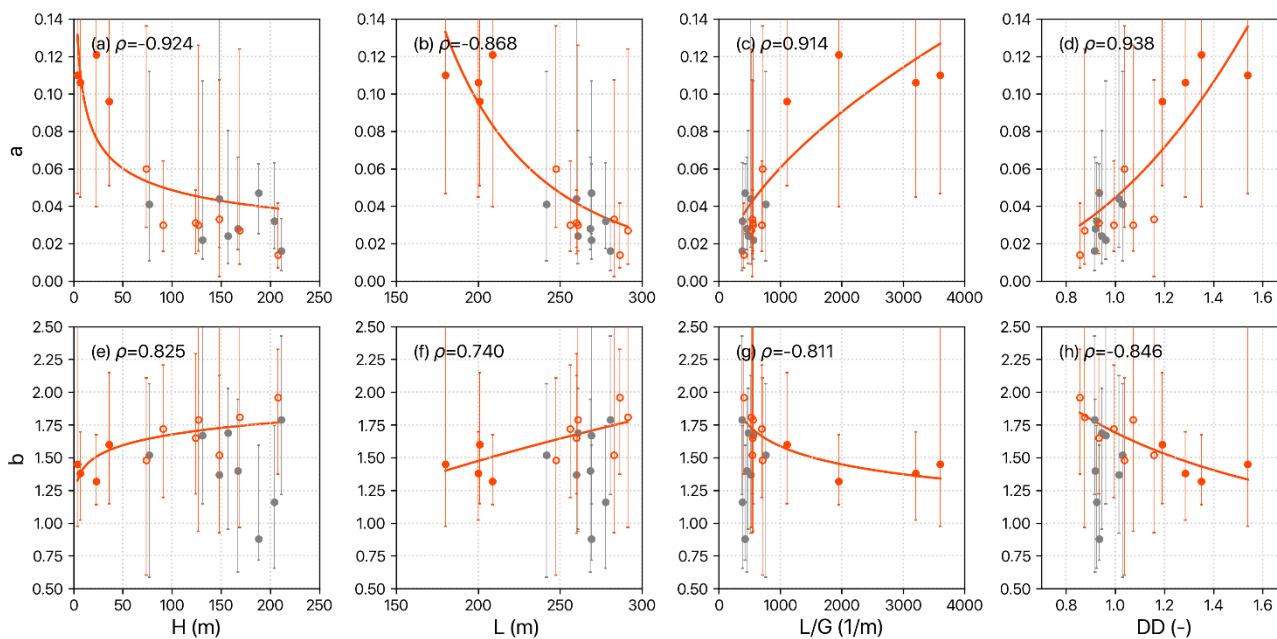
**Figure 7: Scatter plots of the median and range of recession parameters and landscape variables. Orange solid, hollow, and gray dots are catchments of small area with high *L/G* ratio, small area with low *L/G* ratio, and large area, respectively. The solid orange line is the power-law fit for small catchments. The Spearman correlation coefficient (*ρ*) is listed beside the annotation.**
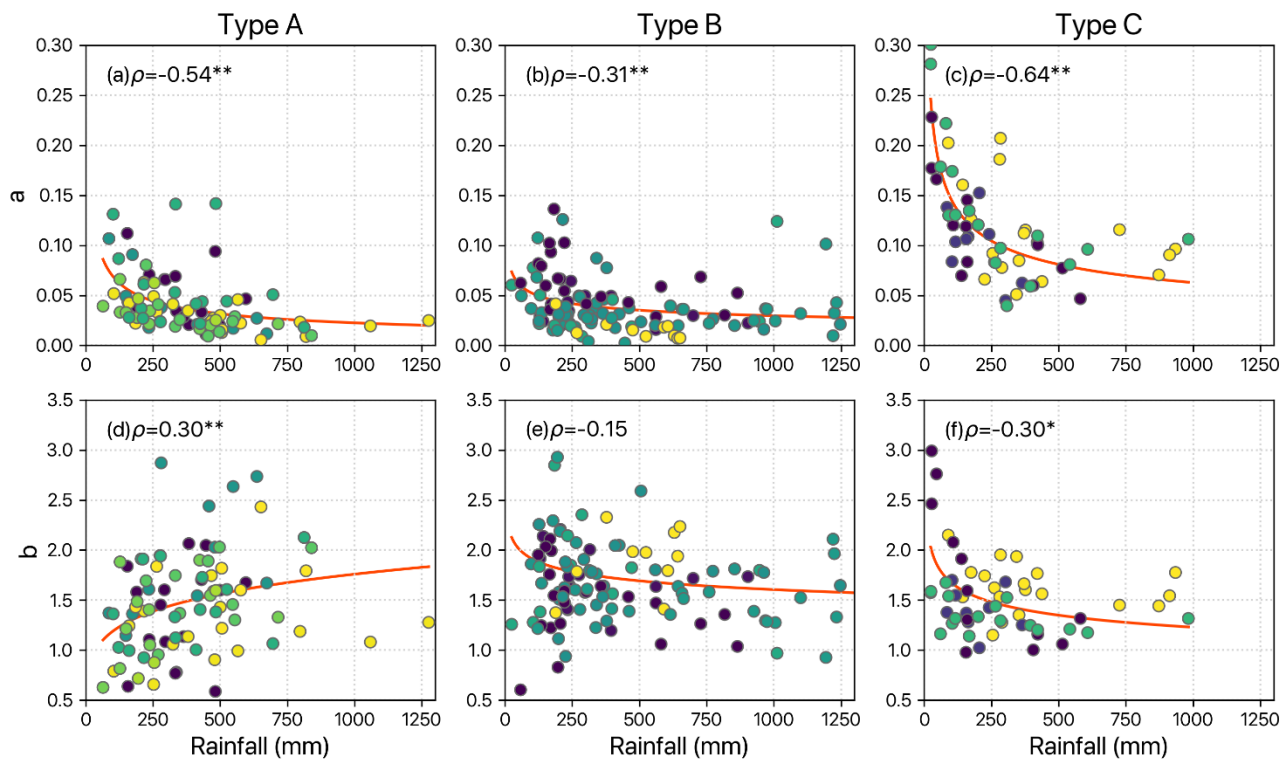
500 **Figure 8: Scatter plots of recession parameters against total rainfall for different catchment types, corresponding to Fig. 6a. Type A is large catchments (area > 500 km²), B is small with low *L/G* ratio catchments, and C is small with high *L/G* ratio catchments. The yellow-green-blue color of dots represents the low to large L/G. The orange line is the exponential fit with spearman correlation coefficient (\* and \*\* means 95% and 99% level of confidence, respectively).**

505
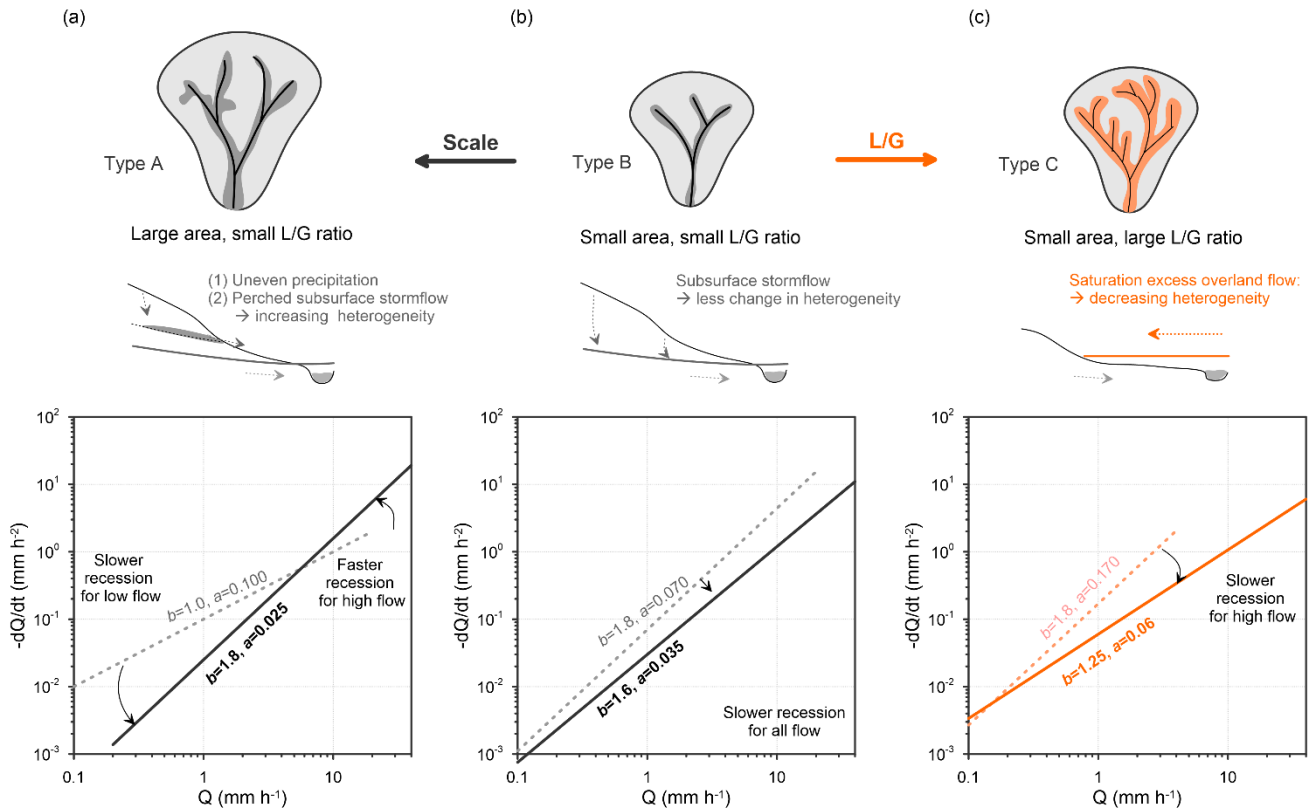
**Figure 9: The conceptual diagram demonstrating the regulation of landscape variables on the direction of the rainfall-recession relationship. The top panel presents the catchment area and the stream network of three landscape types of catchment corresponding to Fig. 6b. The middle panel presents the cross-sectional valley with descriptions of drainage behavior. Here, (a) type A, large and steep slope, drains water via multiple sources of subsurface flow; (b) type B, small**

510 **and steep slope, drains water via fewer sources of subsurface flow; and (c) type C, small and gentle slope, drains via the extension of the saturated zone along the riparian zone. Correspondingly, the recession plots for light (dashed line) and heavy (solid line) rainstorms with their recession parameters are presented on the bottom panel.**